WIND TUNNEL MODELING OF SNOW FENCES AND NATURAL SNOW FENCE CONTROLS

James D. Iversen

Iowa State University
Ames, Iowa 50011

ABSTRACT

Snowdrift modeling research has been carried out in the Iowa State University environmental wind tunnel. As part of this research, a series of experiments were conducted on scale models of snowdrift controls on flat terrain (fences of various porosities and simulated hedgerows and trees). This paper reports primarily on the qualitative aspects of these experiments. The evidence presented illustrates that successful and useful results can be obtained from careful wind tunnel snowdrift modeling experiments.

INTRODUCTION

It is less expensive, quicker, and easier to test a small-scale model of a snow fence or other type of snow accumulator than it is to build a full-scale device for testing with actual blowing snow. The important question remaining for such experiments concerns full-scale predictability from the model test results. Such small-scale models were first tested by Finney (1934, 1937, 1939) in a small wind tunnel; many of the results he obtained are still used in snow fence placement and highway design. Other wind tunnel experiments have been performed by Becker (1944), Nokkentved (1940), Kreutz and Walter (1956), Gerdel and Strom (1961), Strom et al. (1962), Stehle (1964), Sherwood (1967), Brier (1972, Kind and Murray (1980) and by the author (Iversen, 1979b, 1980). Model scale experiments in water have been performed by Theakston (1970), Isyumov (1971), Norem (1975), Calkins (1974, 1975), and de Krasinski et al. (1975, 1979). An interesting and carefully performed set of experiments has been performed recently by Tabler (1980a, 1980b) and Tabler and Jairell (1980) using scale models placed on a frozen lake with natural snow itself used as the modeling material.

The exact similitude requirements for performing scale modeling of drifting snow problems are not met on a small scale because of the large number of modeling parameters that cannot be satisfied simultaneously. Those who have reviewed the similitude requirements include Gerdel and Strom (1961), Odar (1962, 1965), Isyumov (1971), Norem (1975), de Krasinski et al. (1975, 1979), Kind (1976), Iversen (1979a, 1979b, 1980), and Tabler (1980b). The complexity of the similitude problem is emphasized by the fact that, in general, none of these authors agrees as to the most important or appropriate sets of parameters on which to base a similitude.

In 1978 and 1979, snowdrift modeling research in the Iowa State University environmental wind tunnel was carried out under contract to the Iowa Department of Transportation. This research was primarily for the purpose of testing modeling techniques to determine optimum drift control configurations for Interstate Highway grade separation structures (overpass bridges). This work is reported in Ring et al. (1979) and in Iversen (1979b, 1980). In the course of this study, a short series of experiments was conducted on scale models of snowdrift control on flat terrain (fences of various porosities, simulated hedgerows and simulated trees). The purpose of this paper is to report on the qualitative aspects of the flat terrain experiments.

SALTATION MODELING

The transport of snow in the formation of drifts is primarily by means of the so-called saltation mode, rather than by the effects of wind on the falling snow particles before they first hit the ground. Thus, as shown by Iversen (1979a, 1980), the important similitude parameters are groups of original dimensionless parameters formed by consideration of the saltation phenomena, namely, the mass transport rate and equivalent aerodynamic roughness. The transport rate parameter is

$$\left.\frac{\rho U^2}{2\rho_p gH}\left(1-\frac{U_o}{U}\right)\right|_{\text{model}} = \left.\frac{\rho U^2}{2\rho_p gH}\left(1-\frac{U_o}{U}\right)\right|_{\text{full-scale}} \tag{1}$$

The equivalent roughness parameter is

$$\left.\frac{\rho U_*^2}{\rho_p gH}\right|_{\text{model}} = \left. A_1^2 \frac{D_p}{H}\left(\frac{U_*}{U_{*t}}\right)^2\right|_{\text{model}} = \left. A_1^2 \frac{D_p}{H}\left(\frac{U_*}{U_{*t}}\right)^2\right|_{\text{full-scale}} \tag{2}$$

For the flat terrain experiments, the dimensionless time is defined, using Equation (1), as

$$\tilde{t} = \frac{\rho U^2}{2\rho_p gH}\left(1-\frac{U_o}{U}\right)\frac{Ut}{L} \tag{3}$$

A comparison of the different types of control is best done by comparing dimensionless values of drift profile area, drift length, drift plan area or drift volume at equal values of dimensionless time. (For the grade separation experiments, enough additional data were obtained to include the roughness term in the definition of dimensionless time.) The ratio of full-scale to model-scale wind speeds is obtained using Equation (1). Test conditions for the experiments reported in this paper are listed in Table 1.

WYOMING FENCE EXPERIMENTS

Figure 1 shows a typical Wyoming Highway Department snow fence, 3.66 m in height. This particular fence has a 0.1 H gap at the fence bottom, is inclined 15° from the vertical, has alternate 15-cm boards and board spacing, and a porosity of 50%. Figure 2 is an end view of another fence and designer Dr. Ronald Tabler of the U.S. Forest Service. The fence description and its associated drifting characteristics can be found in Tabler (1973, 1974, 1977, 1980a). Additional characteristics of similar snow fences are reported by Tabler and Veal (1971) and Martinelli (1973).

Most of the flat terrain wind tunnel experiments were performed with the 50% porous Wyoming snow fence design, with a miniature fence 2.54 cm in height and 76.2 cm in length (length-scale ratio of 144), to allow comparison with Tabler's full-scale and frozen-lake model data. The material used to simulate snow consisted of glass spheres, of density 3990 kg/m^3, and average particle diameter of 49 μm. The large density of the spheres helps decrease the model value of the parameter of Equation (1), making it easier to simulate full-scale drifts with reasonable full-scale wind speed values. The small particle diameter aids in satisfaction of the parameter of Equation (2), and also in simulating the capability of real snow to form cornices. The friction caused by the wind blowing over the particles and then moving them results in the particles becoming electrostatically charged. This electrostatic charge results in a temporary angle of repose much greater than the usual 34°. For snow, the larger angle of repose (which can, of course, be greater than 90°)

Table 1. Test conditions for wind tunnel experiments illustrated in Figures 3-23.

Run Number	U, Speed at Fence or Bridge Height H (m/s)	Parameter of Equation (1)	Ratio, Full-Scale to Model-Scale Speed
10-14-1	5.5	0.0070	3.8
10-25-1	6.2	0.0156	4.8
12-7-1	5.1	0.0064	3.9
12-9-1	5.2	0.0068	3.9
12-21-1	5.6	0.0075	3.8
1-20-1	4.7	0.0079	4.7
1-20-2	3.6	0.0037	4.2
1-22-1	3.7	0.0039	4.2
1-22-2	3.8	0.0043	4.3
1-29-1	3.3	0.0030	4.1
1-31-1	3.5	0.0036	4.3
1-31-2	3.3	0.0029	4.1
2-3-1	4.2	0.0061	4.6
2-6-1	3.5	0.0035	4.2
5-1-1	3.0	0.0019	3.7
5-8-1	3.7	0.0037	4.1
5-10-1	4.1	0.0051	4.3

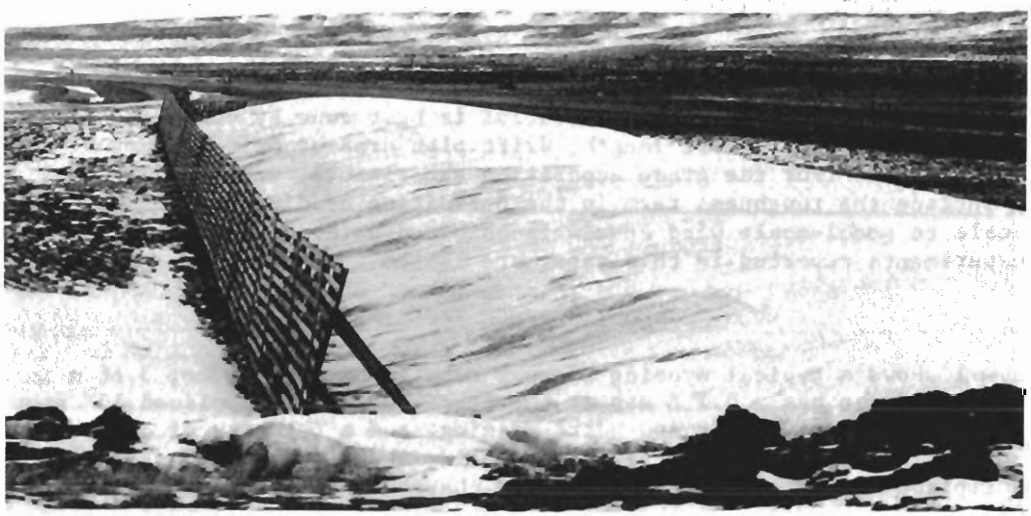

Fig. 1. Wyoming highway 3.66 m snow fence. (Note the almost-complete lack of upwind drift and the near-equilibrium downwind drift. Photograph by author, February 1979, Interstate 80, Elk Mountain Interchange.)

is permanent, due to inter-particle sintering. For the glass spheres, after a test is completed, gradual disappearance of the charge results in a return to the normal 34° angle of repose and avalanching occurs, as illustrated in Fig. 3. Cornice formation simulation is not possible with spheres that are much larger, because the charge cannot be held for a sufficient length of time.

Successive stages of development of the downwind drift are shown in Figs. 4-10. The cornice, while not quite as sharp-edged as in a full-scale snow, is readily apparent for

Fig. 2. Wyoming highway 3.66 m snow fence and designer Dr. Ronald Tabler. (Note significant upwind drift.)

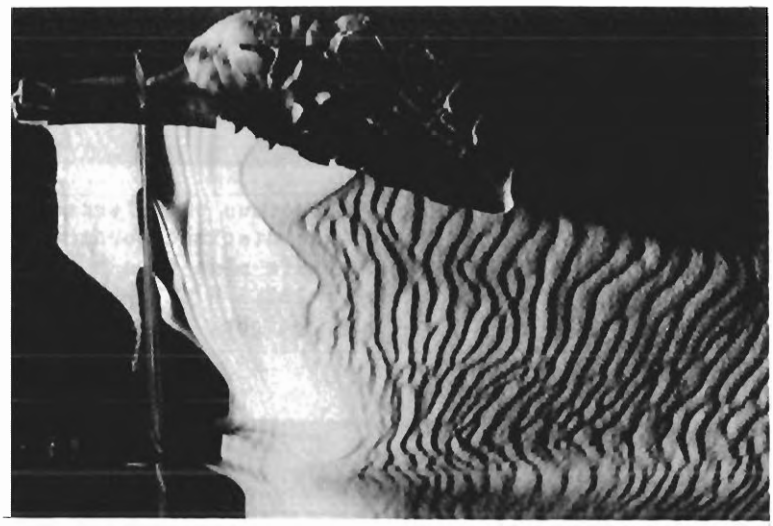

Fig. 3. Wind tunnel simulation of 50% porous snow fence, Run 5-10-1, flow left to right. Notice avalanche of glass spheres (see text).

intermediate stages of development in Figs. 4 and 5. Close-up views of the cornice formation in Fig. 4 are shown in Figs. 6 and 8. The near-equilibrium drift, is shown in Figs. 7 and 9. Note that the cavity downwind of the cornice has been filled so that the cornice no longer exists.

The development in plan of the downwind drift is shown in Fig. 10. Unevenness of the floor surface caused a variation in gap height laterally along the fence. Where the gap is smallest, the downwind drift lies closest to the fence. The fence supports also affected the lateral drift uniformity. The asymmetry, with the longer portion of the drift on the right end of the fence, is probably caused by a slight nonuniformity in tunnel speed across the test section. The nonuniformity in drift profile was not as great as might be indicated from the plan views. The final drift profile was measured at five lateral points along the fence with the profiler shown in Fig. 7. The average of these five profiles is shown in Fig. 11 as the solid triangle data points. The comparison with Tabler's (1977, 1980a, 1980b) full-scale data is considered to be good. The upwind portion of the drift is below the full-scale data, probably because the effective wind speed is higher for the model than it is at all times for the full-scale fences. There is evidence to indicate that the higher the wind speed, the farther from the fence the drift begins to be established. The

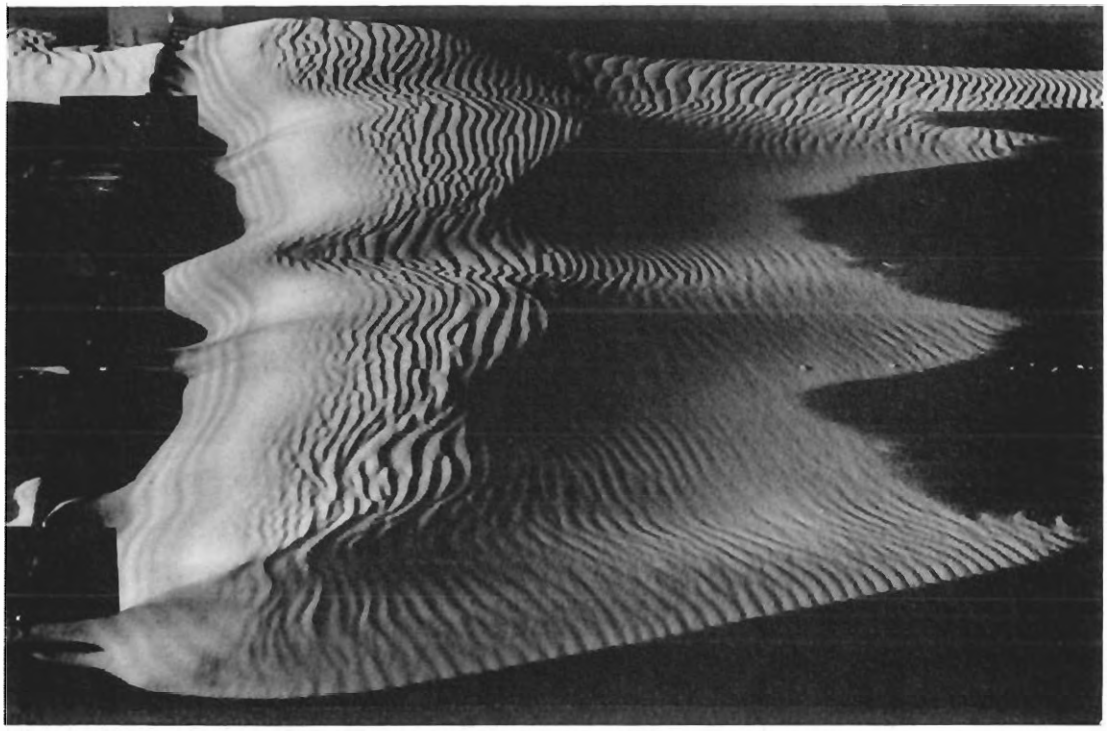

Fig. 4. Wind tunnel simulation of 50% porous snow fence, Run 5-1-1, flow left to right. Notice the distinct cornice formation. Dimensionless time = 375.5, drift plan area = 422.6 H^2, profile area = 10.1 H^2, volume $\cong$ 265.5 H^3. Fence is 0.762 m long and measures 0.0254 m in height.

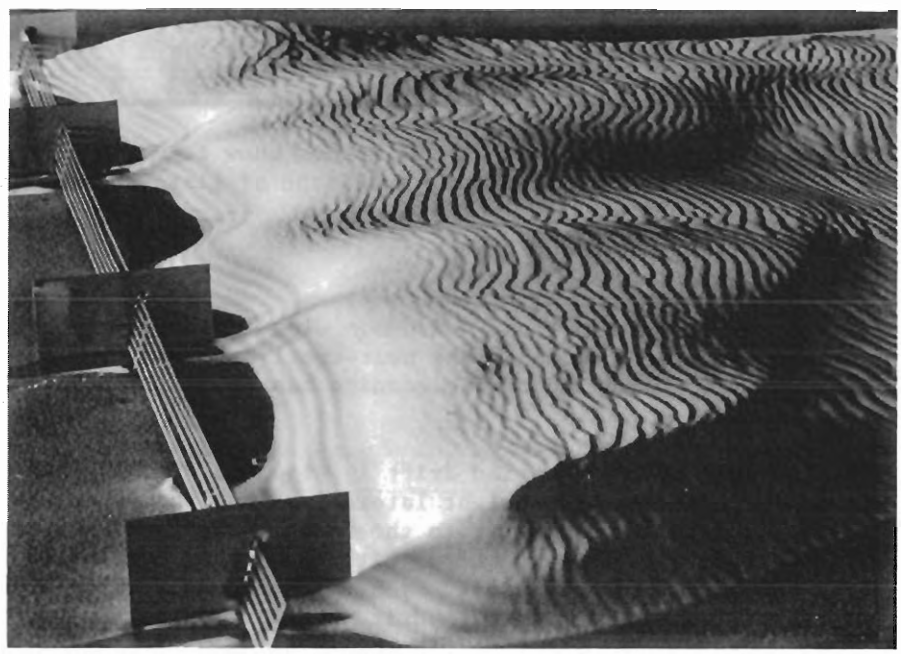

Fig. 5. Wind tunnel simulation of 50% porous snow fence, Run 5-8-1, flow left to right, cornice farther downwind. Dimensionless time = 999.3, drift plan area = 553 H^2, profile area = 14.65 H^2, volume $\cong$ 365.9 H^3.

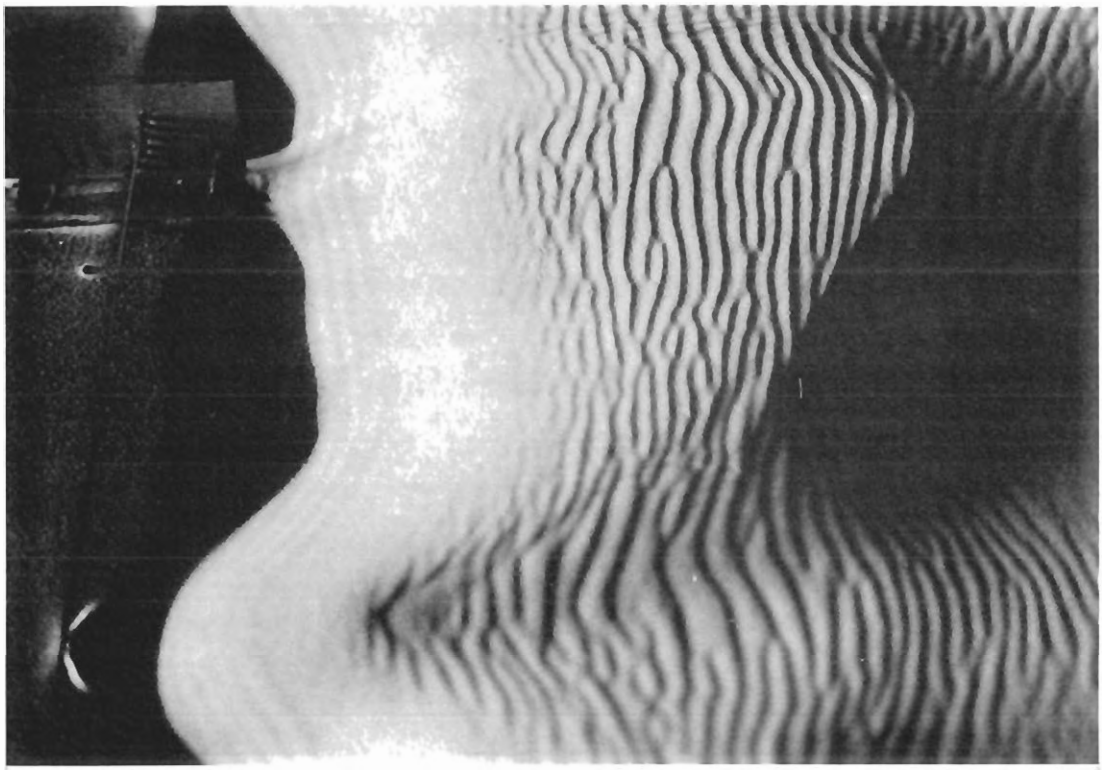

Fig. 6. Close-up view of cornice formation, Run 5-1-1. Dimensionless time = 375.5, flow left to right.

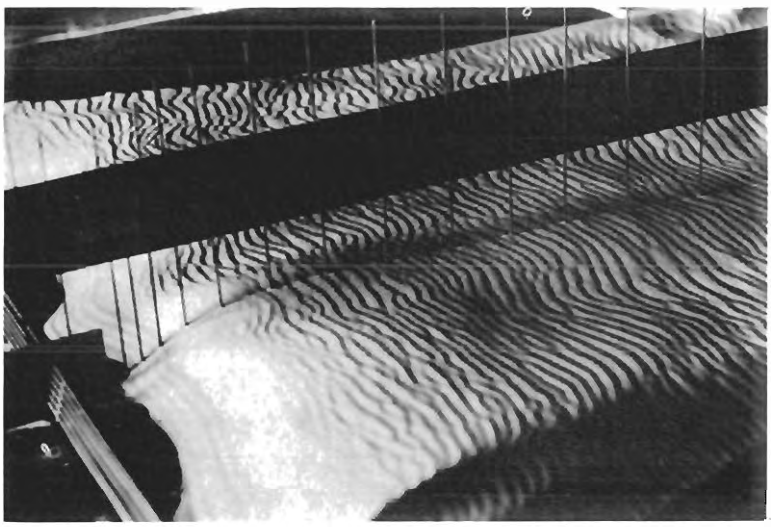

Fig. 7. View of drift profiler used to measure drift profile after a wind tunnel run. During the run, the profile is measured photographically.

Fig. 8. Close-up view of cornice formation and edge of drift, Run 5-1-1, flow left to right. The ripple pattern, of course, is not to scale. Ripple wave length is sufficiently short so that gross drift features are not affected except, perhaps, near the cornice.

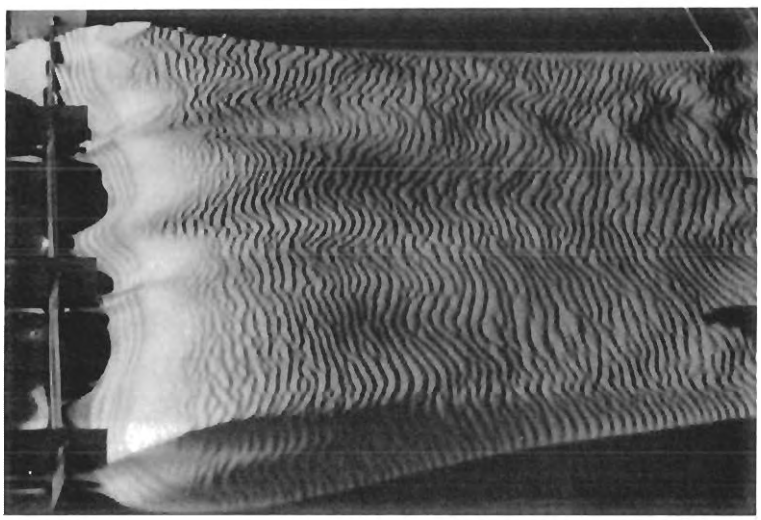

Fig. 9. Wind tunnel simulation of 50% porous snow fence, Run 5-10-1, flow left to right. Drift is near equilibrium and cornice has disappeared. Dimensionless time = 1294.7, drift area = 644.9 H^2, profile area = 16.76 H^2, volume = 404.6 H^3.

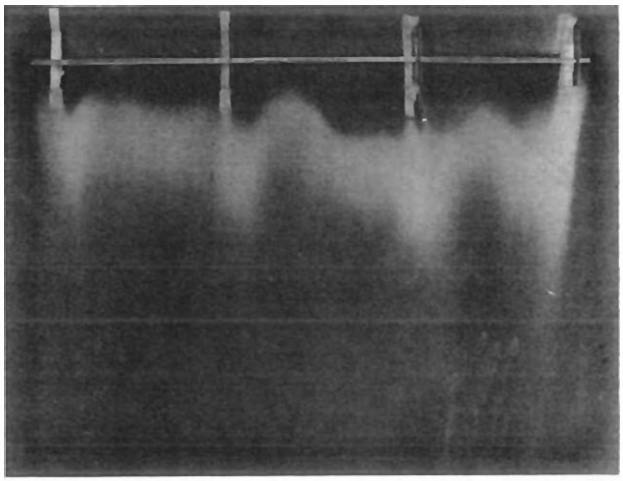

a. A few seconds after wind on, Run 5-1-1.

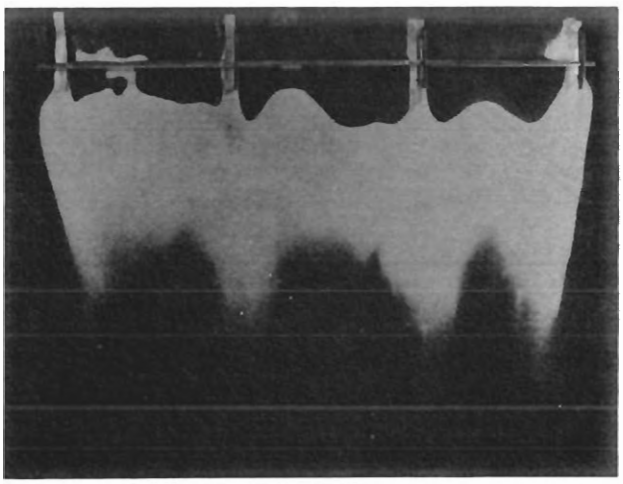

b. Run 5-1-1, time = 52 minutes (dimensionless 39.4), plan area = 259.6 H^2, volume $\cong$ 11.52 H^3.

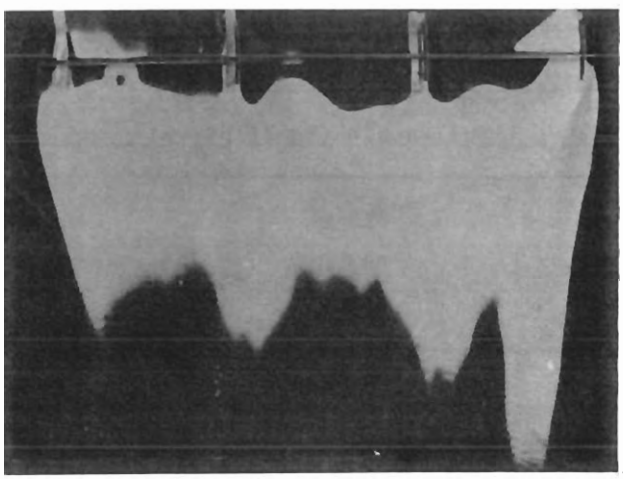

c. Run 5-1-1, time = 257 minutes (dimensionless 194.6), plan area = 360.7 H^2, volume $\cong$ 128.2 H^3.

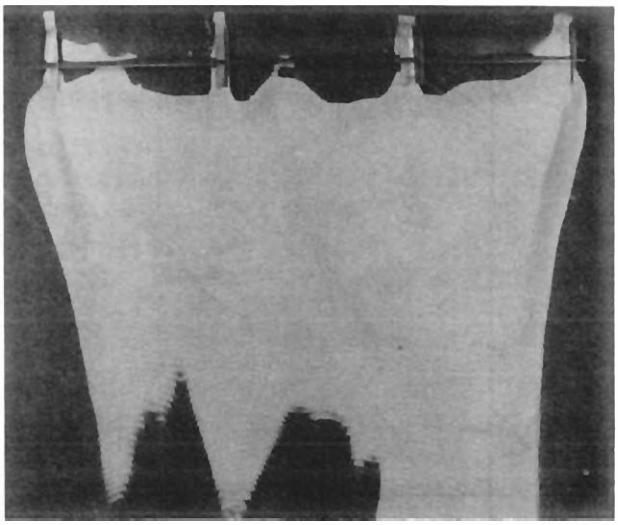

d. Run 5-8-1, total time = 848 minutes (dimensionless 999.3), plan area = 553 H^2, volume $\cong$ 365.9 H^3.

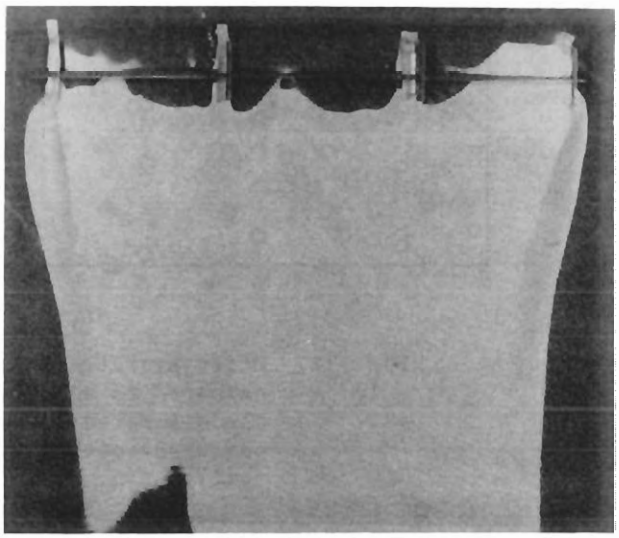

e. Run 5-10-1, total time = 958 minutes (dimensionless 1294.7), plan area = 644.9 H^2, volume $\cong$ 404.6 H^3.

Fig. 10. Plan views of 50% porous snow fence simulation. Asymmetries are due to uneveness in floor (80 grit sandpaper), fence supports, and perhaps slight nonuniformity in tunnel speed.

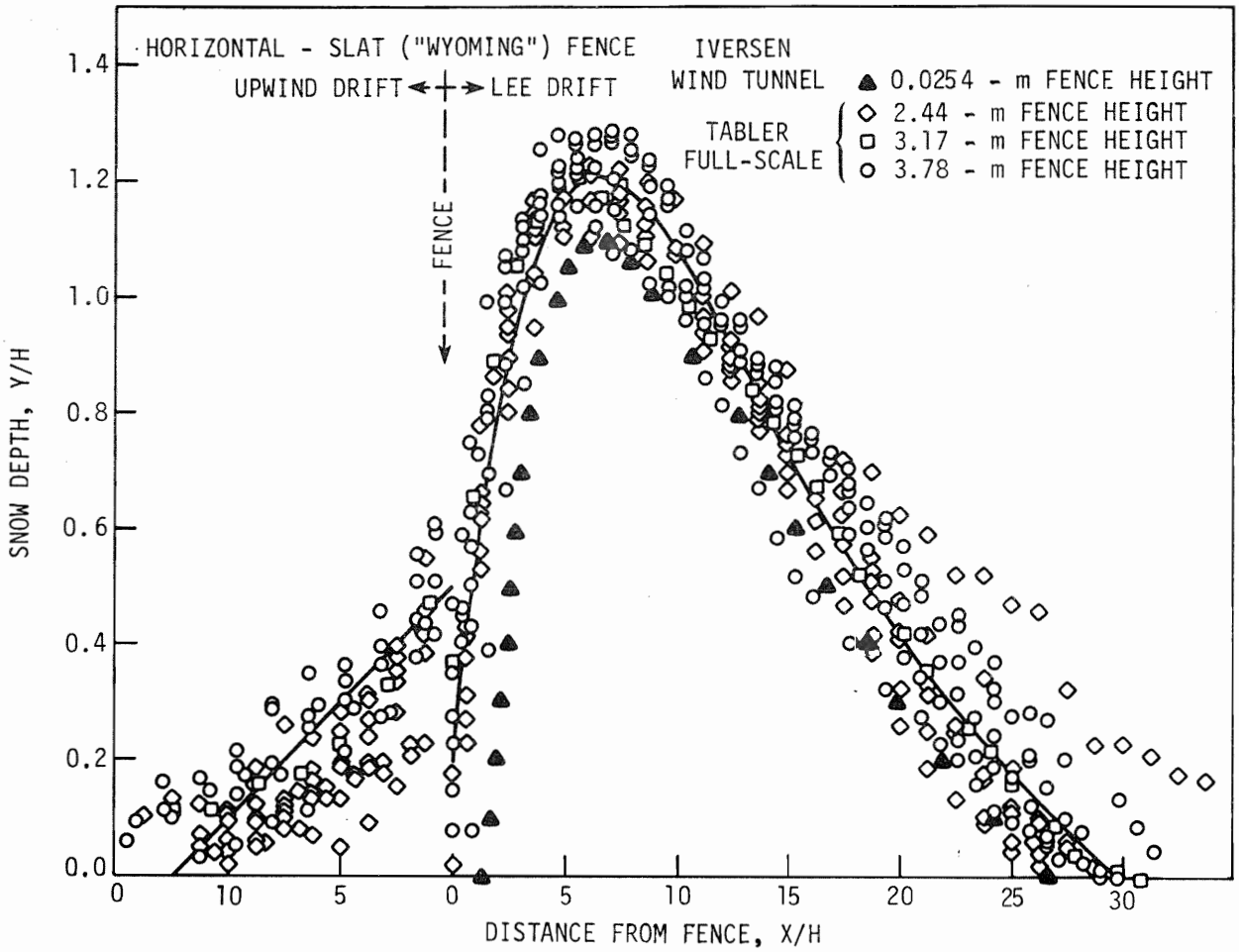

Fig. 11. Drift profiles: Full-scale measurements from Tabler (1980a) compared to wind tunnel simulations for the 50% porous fence. The simulated downwind drift profile compares well in size and shape with the full-scale, except near the fence (see text).

Table 2. Comparison of wind tunnel and full-scale downwind drifts for Wyoming 50% porous fence.

	Wind Tunnel ($\tilde{t}$ = 1295)	Full-scale (Equilibrium)
Profile Area	17.2 H^2	18 H^2
Plan Area	645 H^2	693 H^2
Volume	405 H^3	465 H^3

model drift has probably not reached equilibrium (sometimes called saturation). The downwind portion of the drift is within the full-scale data scatter and has the same slope as Tabler's fitted average profile curve. Comparison of full-scale (Tabler, 1979) and wind tunnel measurements are made in Table 2.

HEDGEROW AND OTHER FENCE EXPERIMENTS

Several other types of drift controls were tested on flat terrain. Results from a fence of 25% porosity are shown in Fig. 12. The effect of fence bottom gap is quite noticeable in this mismounted model, both on the upwind and downwind drifts. The effect of the gap obviously is to increase the fence holding capacity. Plan views of solid fences, with and without a bottom gap, are shown in Fig. 13. The difference in downwind drift planform shape due to control porosity is striking, with the wake due to a solid fence causing a planform shape quite different from the partially porous controls of Figs. 10, 12, and 14. The fact that air cannot flow through the solid fence causes a much greater pressure difference between the upwind and downwind sides of the fence. Thus, there is a tendency for air to flow around and up over the ends of the fence, causing swirling flows that carry material downstream rather than permitting deposition as in the center of the wake. The effect of the gap (Figs. 13d,e,f) is to cause more deposition downwind very early and less deposition upwind of the fence. The gap eventually becomes plugged, after which there is little or no difference between the two solid fence control systems.

Plan views of tests of a simulated hedgerow and another 50% porous fence (at a higher speed than for Figs. 4-11) are illustrated in Fig. 14. A thick sufficiently porous hedgerow can cause a significant amount of drifting both upwind and downwind of the row. The wind speed for the 50% porous fence in Figs. 14d,e,f was higher than for Fig. 10, causing material to be deposited initially farther downwind from the fence. Flow speed uniformity and gap uniformity were slightly better in this experiment than for the experiments of Figs. 3-10.

Profile views, showing the differences in upwind and downwind drift shapes among the various control types, are shown in Fig. 15. Figures 15a,b,c,d clearly show the edge of the thick separated flow region due to the visibility of the paths of the simulated snow particles. The contrast with Fig. 15e is great, with almost all particles traveling through the porous fence rather than over it. Figure 15g shows that for only 25% porosity, a significant amount of material is going over the fence as well as through it. In Fig. 15j, for the solid fence with bottom gap, the gap is still clear and quite a bit of material is shooting under the gap as well as over the fence. In these experiments, except for Fig. 15ℓ, wind tunnel run time was far too short to approach equilibrium drift. Thus, strict comparisons of the various controls could not be made. For early times at least, however, the 50% fence is superior (volume vs time).

Aerial photographs of tree row and hedgerow drifts are shown in Figs. 16 and 17. It is interesting to compare Fig. 17 with Fig. 14a and b, and Fig. 16 with Fig. 18. The model guardrail in Fig. 19 is only 5.08 mm in height, indicating that very small realistic model drifts with sharp-edged cornices can be formed with these glass spheres in a boundary layer wind tunnel.

a. Run 1-31-2, time = 1 minute (dimensionless = 1.25), plan area = 91.5 H^2.

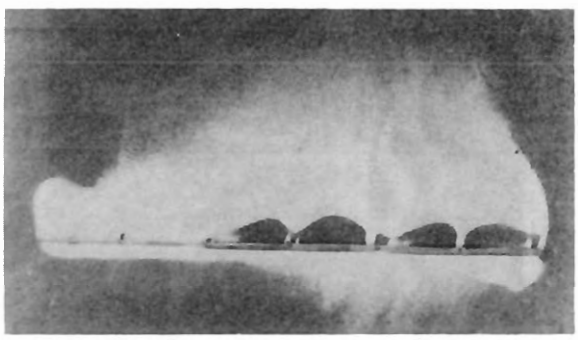

b. Time = 13 minutes (dimensionless = 16.23), plan area = 201 H^2, volume $\tilde{=}$ 22.6 H^3.

Fig. 12. Plan views of 25% porous snow fence simulation, flow bottom to top. The effect of fence bottom gap is illustrated very clearly. The mismounted model has no gap for the left one-third of the fence and approximately 10% fence height gap on the right two-thirds.

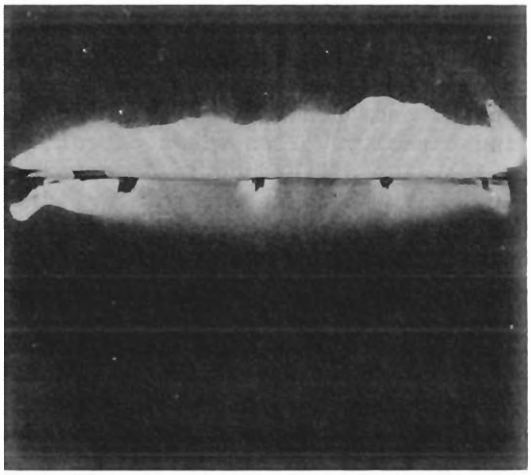

a. Run 1-20-2, time = 5 minutes (dimensionless = 11.0), plan area = 210 H^2, no gap.

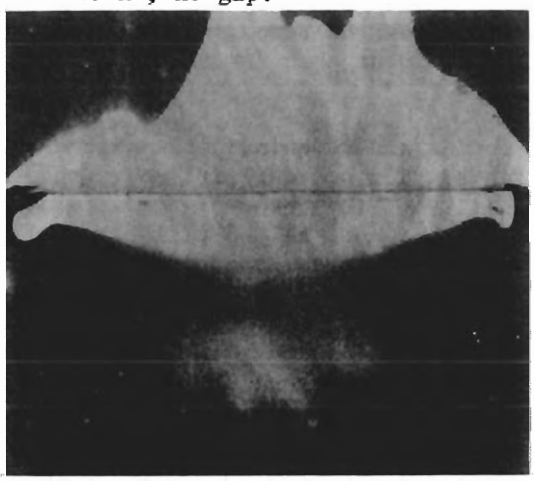

b. Run 1-20-2, time = 26 minutes (dimensionless = 57.0), plan area = 411 H^2, no gap.

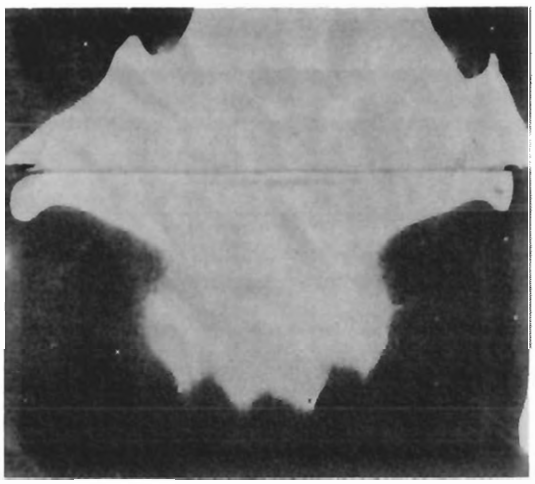

c. Run 1-20-2, time = 49 minutes (dimensionless = 107.4), plan area = 609 H^2, no gap.

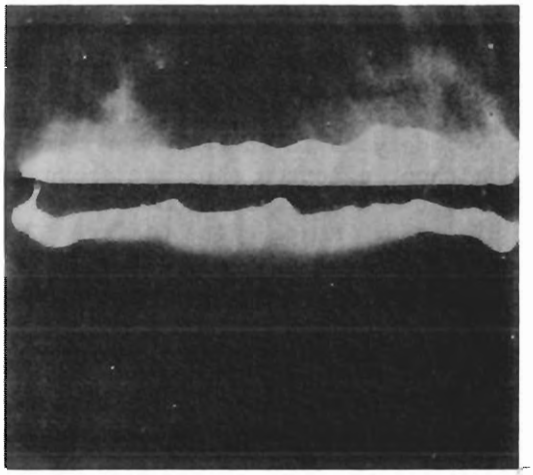

d. Run 1-22-1, time = 3 minutes (dimensionless = 5.4), plan area = 163.5 H^2, 10% gap.

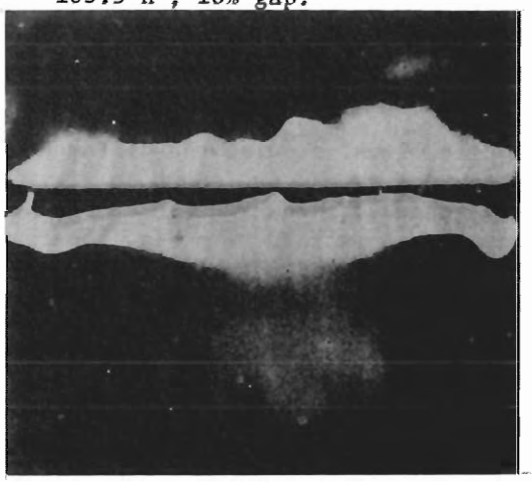

e. Run 1-22-1, time = 15 minutes (dimensionless = 27.2), plan area = 204.1 H^2, volume $\tilde{=}$ 45.94 H^3, 10% gap.

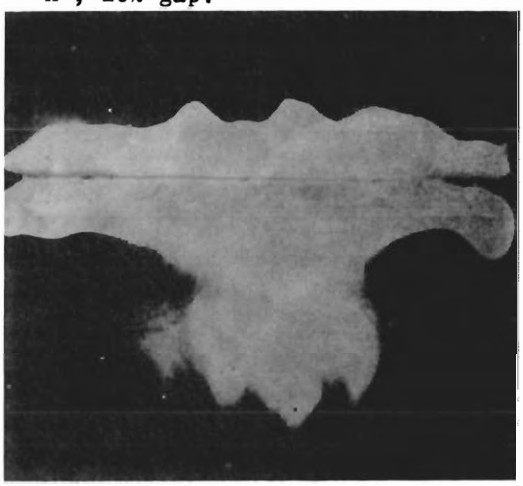

f. Run 1-22-1, time = 51 minutes (dimensionless = 92.5), plan area = 335.2 H^2, volume $\tilde{=}$ 61.7 H^3, 10% gap.

Fig. 13. Plan views of solid fence simulations with and without 10% bottom gap, flow top to bottom.

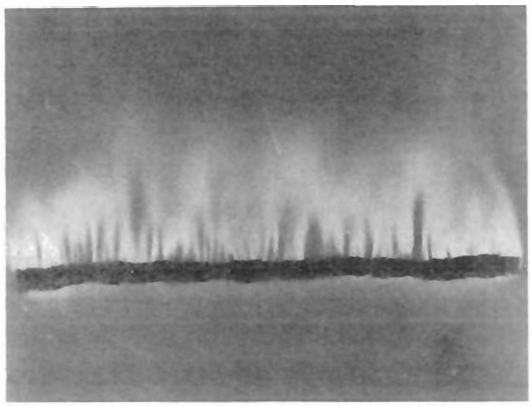

a. Run 1-31-1, time = a few seconds after wind on.

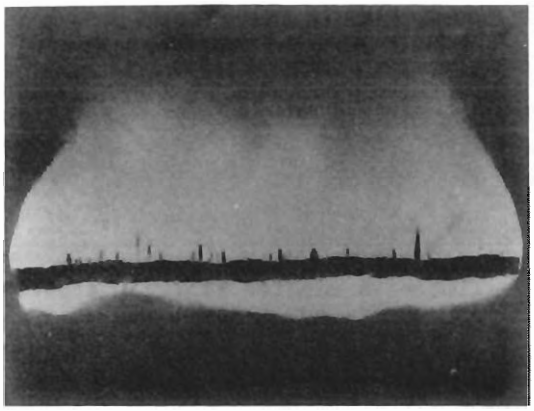

b. Run 1-31-1, time = 4 minutes (dimensionless = 6.4), plan area = 276 H^2.

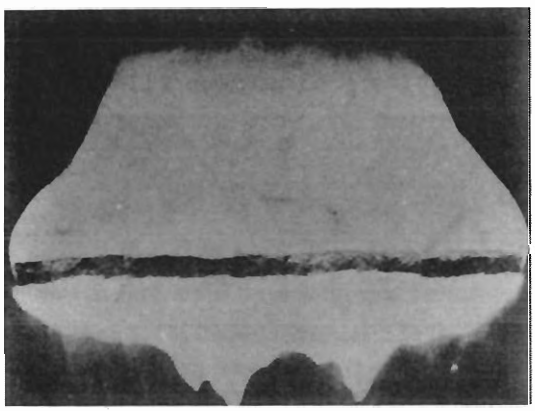

c. Run 1-31-1, time = 30 minutes (dimensionless = 47.4), plan area = 435 H^2, volume $\tilde{=}$ 69.8 H^3.

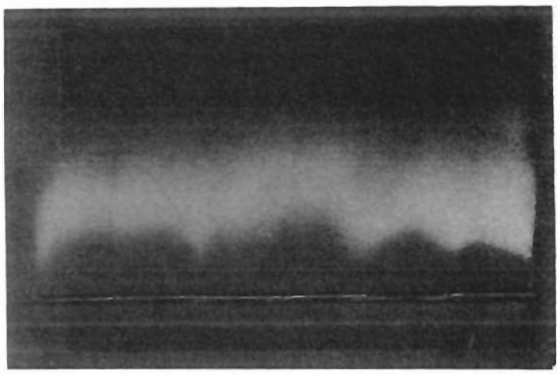

d. Run 1-29-1, time = 1 minute (dimensionless = 1.3).

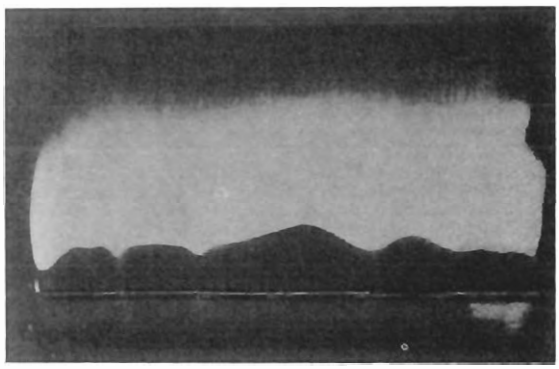

e. Run 1-29-1, time = 13 minutes (dimensionless = 16.5), plan area = 247 H^2, volume $\tilde{=}$ 8.6 H^3.

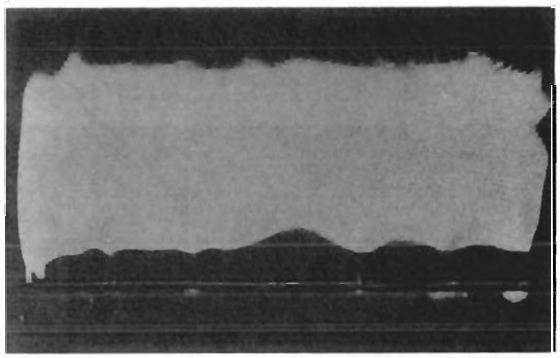

f. Run 1-29-1, time = 60 minutes (dimensionless = 76.1), plan area = 339 H^2, volume $\tilde{=}$ 142.9 H^3.

Fig. 14. Plan views of simulated hedgerow (a, b, c) and 50% porous fence simulation (d, e, f), flow bottom to top.

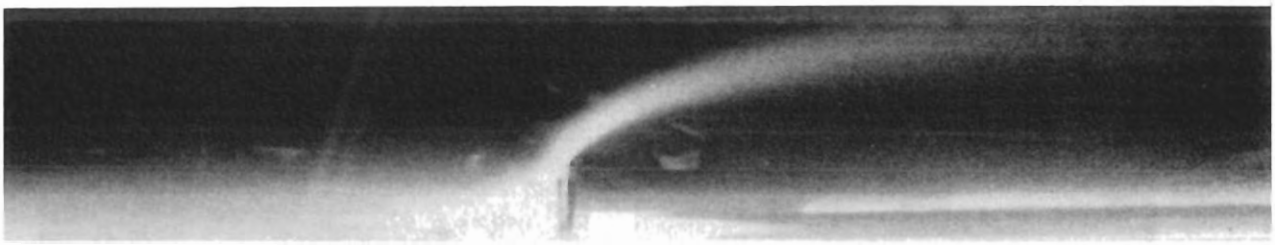

a. Run 1-20-1, solid fence without gap. Time = 4 minutes (dimensionless = 18.9).

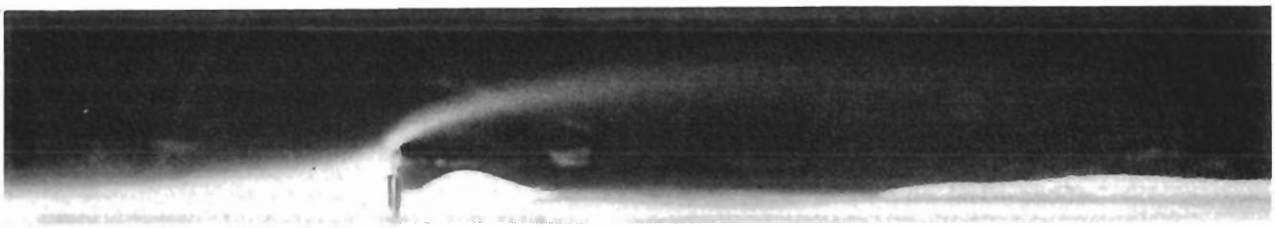

b. Run 1-20-2, solid fence without gap. Time = 42 minutes (92.1).

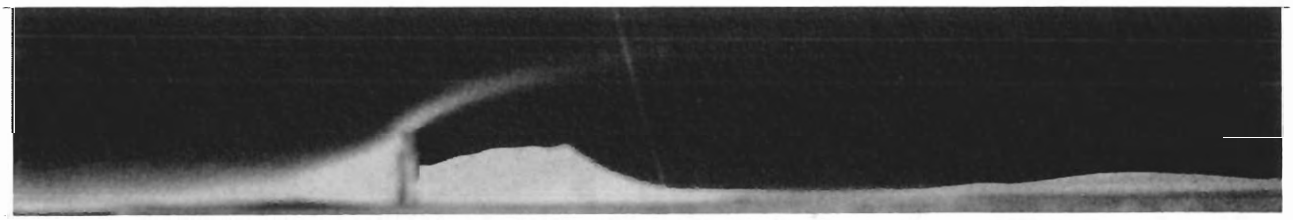

c. Run 1-22-1, solid fence with gap. Time = 76 minutes (137.9), profile area = 3.0 H^2, volume $\cong$ 98.7 H^3.

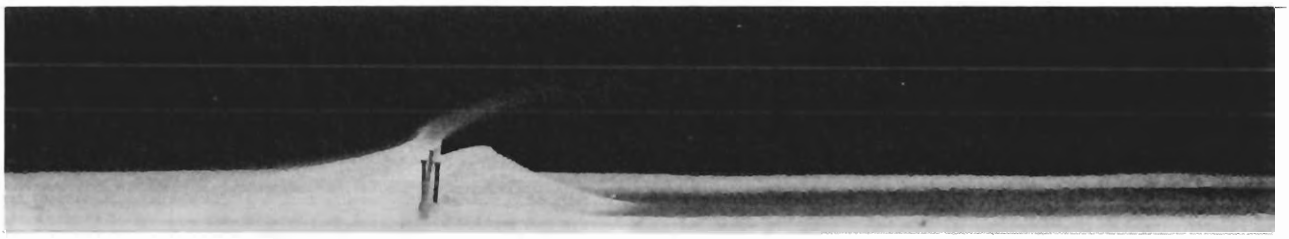

d. Run 1-22-2, solid fence with gap. Time = 65 minutes (134.4).

e. Run 1-29-1, 50% porous fence. Time = 111 minutes (140.8), profile area = 7.3 H^2, volume $\cong$ 98.4 H^3.

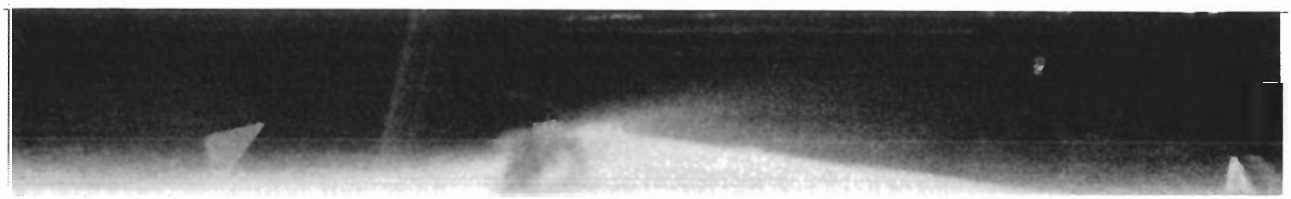

f. Run 1-31-1, simulated full-width hedgerow. Time = 49 minutes (78.8), profile area = 6.1 H^2, volume $\cong$ 153 H^3.

Fig. 15. Profile elevations.

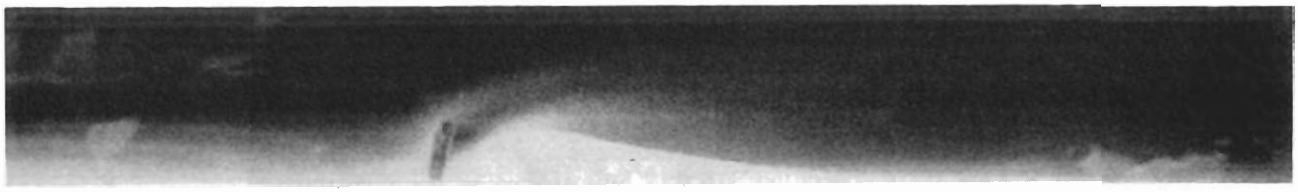

g. Run 1-31-2, 25% porous fence. Time = 91 minutes (113.6), profile area = 3.9 H^2, volume $\cong$ 36.3 H^3.

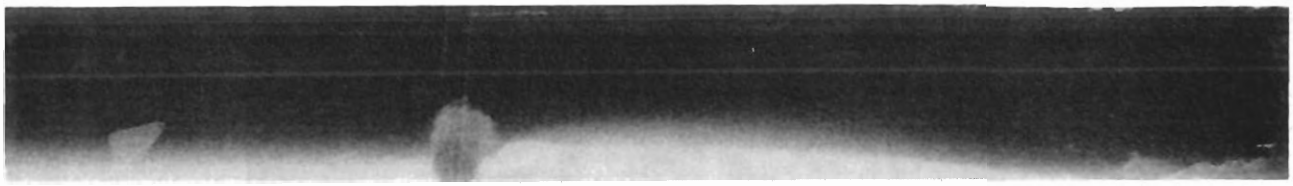

h. Run 2-3-1, simulated half-width hedgerow. Time = 41 minutes (132.7), profile area = 7.1 H^2, volume $\cong$ 207 H^3.

i. Run 2-3-1, simulated half-width hedgerow. Time = 42 minutes (135.9).

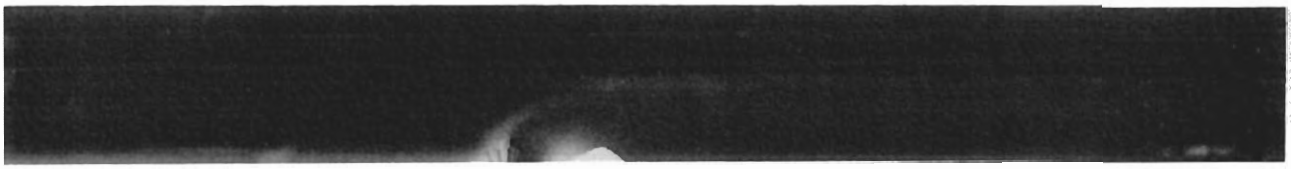

j. Run 2-6-1, solid fence with gap. Time = 121 minutes (189.5), profile area = 2.28 H^2, volume $\cong$ 60.6 H^3.

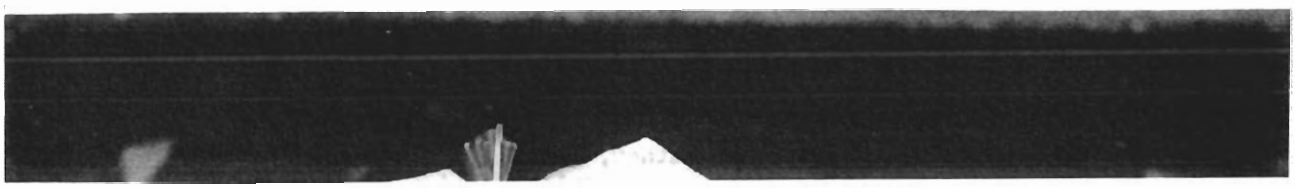

k. Run 2-6-1, solid fence with gap. Time = 140 minutes (219.3), profile area = 2.38 H^2, volume $\cong$ 78.6 H^3.

l. Run 5-8-1, 50% porous fence. Time = 848 minutes (999.3), profile area = 14.65 H^2, volume $\cong$ 365.9 H^3.

Fig. 15. Profile elevations. (Concluded).

Fig. 16. Aerial photograph (by author, 1979) of drifts associated with row of trees (rather porous, particularly near surface).

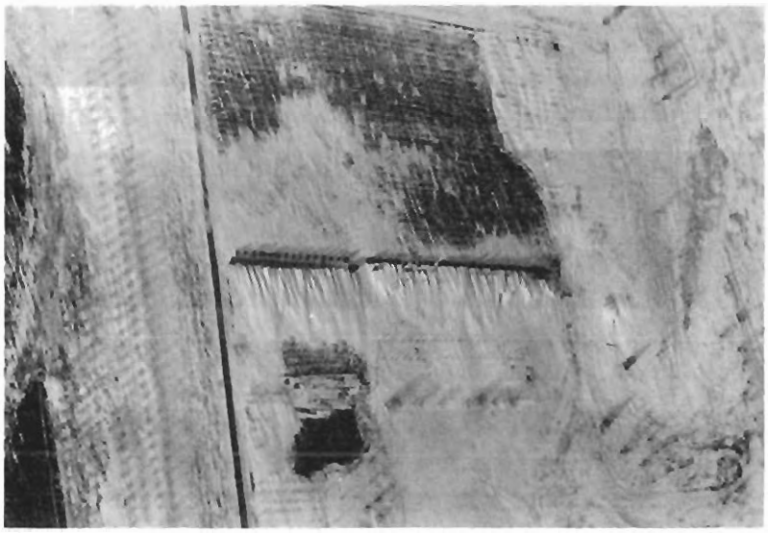

Fig. 17. Aerial photograph (by author, 1979) of drifts associated with dense hedgerow, similar to simulated hedgerow.

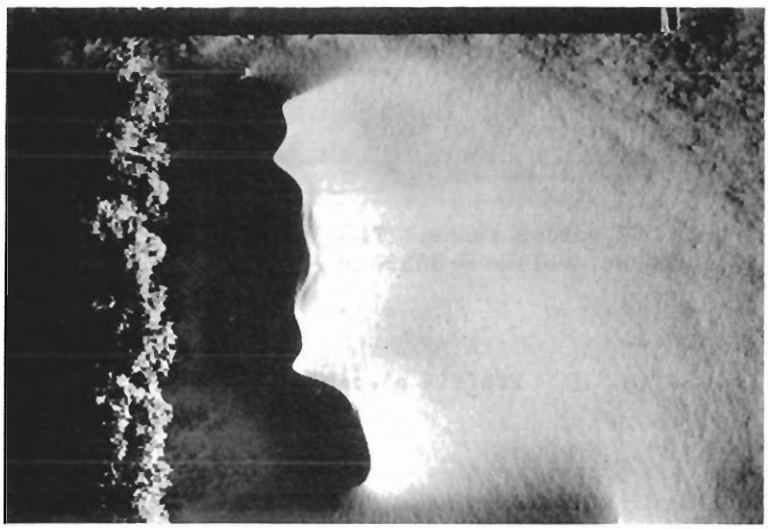

Fig. 18. Run 10-25-1, short simulated row of trees (scale is 0.3 m long), flow left to right.

Bridge model experiments are illustrated in Figs. 20-23. Figures 20 and 21 show drift formation on uncontrolled roadway. Drift formations with simulated hedgerow control are shown in Figs. 22 (poor control) and 23 (good control).

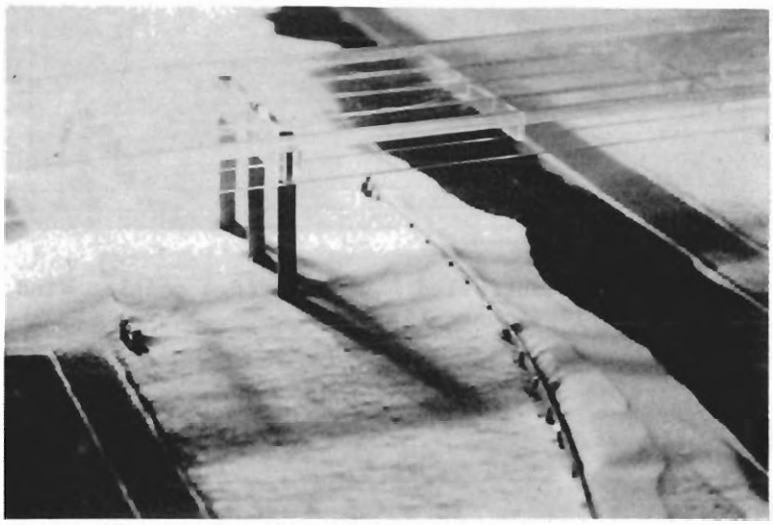

Fig. 19. Photograph of 1/120-scale interstate bridge and guardrail. Note guardrail drift.

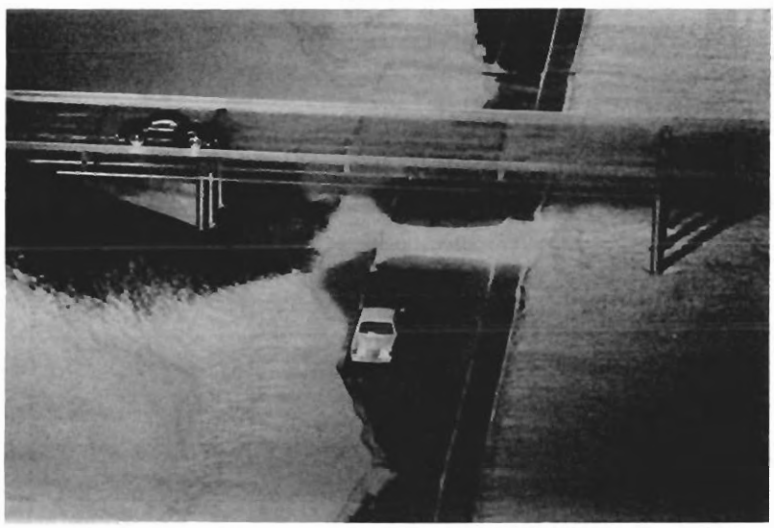

Fig. 20. Run 10-14-1, uncontrolled highway bridge model. Wind direction parallel to bridge centerline.

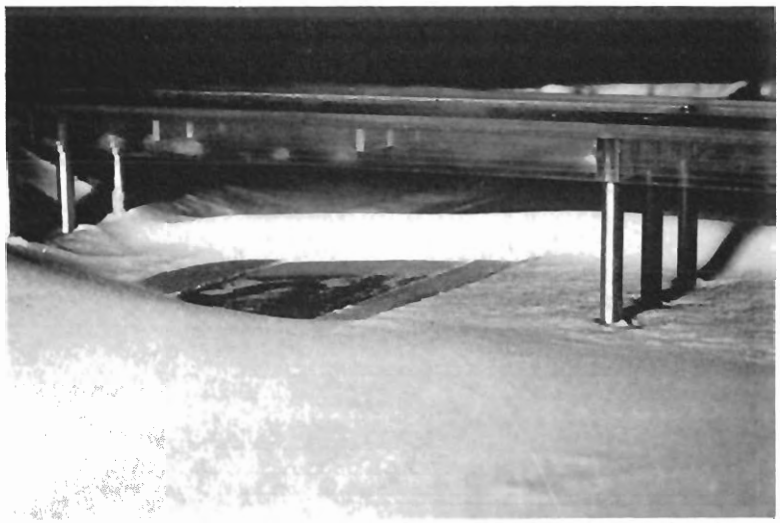

Fig. 21. Run 12-7-1, uncontrolled highway bridge model. Wind direction at 20° to bridge centerline.

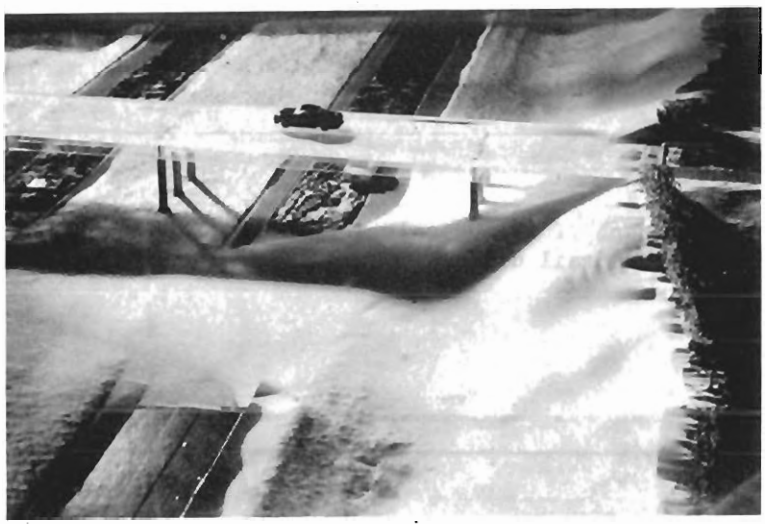

Fig. 22. Run 12-9-1, simulated hedgerow and bridge model (control too close to roadway). Wind direction at 20° to bridge centerline.

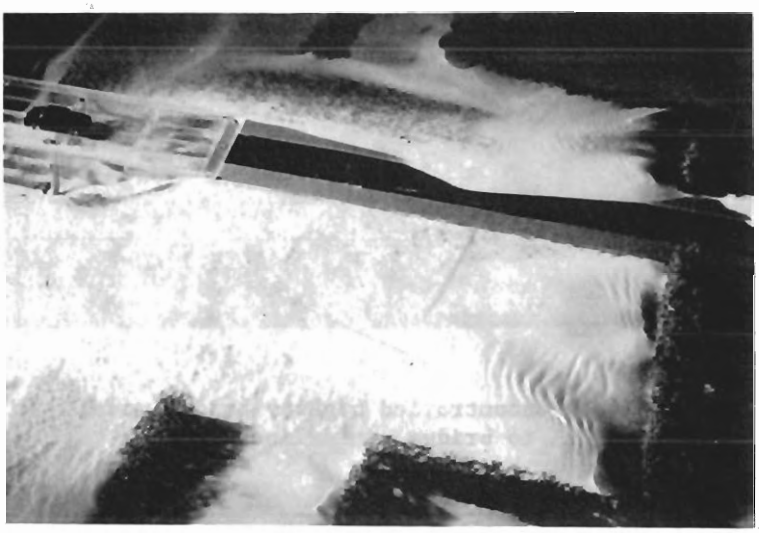

Fig. 23. Run 12-21-1, simulated hedgerow and bridge model. Wind direction at 20° to bridge centerline.

CONCLUSIONS

The boundary layer wind tunnel can be an extremely useful tool in the design and analysis of snowdrift control. The disadvantages of the water channel are: a) the particle-to-fluid density ratio is so small that it is extremely difficult to satisfy the model parameter of Equation (1), and b) the electrostatic effects for cornice formation are absent in water. Because of the former disadvantage, channel bed forms (ripples and dunes) will often obscure the terrain drift features in a water channel. Also, the effective full-scale/model-scale speed ratio is about 30 times higher in water than in air for similar length scale ratios. The photographs and the comparison shown in Fig. 11 present qualitative and quantitative evidence that successful and useful results can be obtained from careful wind tunnel snowdrift modeling experiments.

ACKNOWLEDGMENT

This research was supported by the Iowa Department of Transportation and the Engineering Research Institute of Iowa State University. The author gratefully acknowledges many helpful discussions with Professor Stanley Ring, Professor James Sinatra, and Mr. Jeffrey Benson. Thanks is also due to research assistant V. Ethiraj and technical assistants Cory Wandling and Rory Deichert.

LIST OF SYMBOLS

A_1	Dimensionless threshold friction speed, $U_{*t}(\rho/\rho_p g D_p)^{1/2}$
D_p	Particle diameter
g	Gravitational acceleration
H	Reference height (fence or bridge)
L	Reference length (fence or bridge)
t	Time
$\tilde{t}$	Dimensionless time
U	Undisturbed wind speed at reference height
U_o	Threshold value of U
U_*	Surface friction speed
U_{*_t}	Threshold value of U_*
ρ	Air density
ρ_p	Particle density

REFERENCES

Becker, A. (1944). Natural Snow Fences Along Roads. Bautechnik, 22, 37-42.

Brier, F. W. (1972). Snowdrift Control Techniques and Procedures for Polar Facilities. Technical Report R767, Naval Civil Engineering Laboratory, Port Hueneme, California.

Calkins, Darryl J. (1974). Model Studies of Drifting Snow Patterns at Safeguard Facilities in North Dakota. Technical Report 256, Cold Regions Research and Engineering Laboratory, Hanover, New Hampshire.

Calkins, D. J. (1975). Simulated Snowdrift Patterns. Special Report 219, Cold Regions Research and Engineering Laboratory, Hanover, New Hampshire.

de Krasinski, J. S. and W. A. Anson. (1975). A Study of Snowdrifts Around the Canada Building in Calgary. University of Calgary, Department of Mechanical Engineering, Report No. 71.

de Krasinski, J. and T. Szuster. (1979). Some Fundamental Aspects of Laboratory Simulation of Snow or Sand Drifts Near Obstacles. University of Calgary, Department of Mechanical Engineering, Report No. 151.

Finney, E. A. (1934). Snow Control on the Highway. Bulletin No. 57, Michigan Engineering Experiment Station, East Lansing, Michigan.

Finney, E. A. (1937). Snow Control by Tree Planting, Part VI, Wind Tunnel Experiments on Tree Plantings. Bulletin No. 75, Michigan Engineering Experiment Station, East Lansing, Michigan.

Finney, E. A. (1939). Snow Drift Control by Highway Design. Bulletin No. 86, Michigan Engineering Experiment Station, East Lansing, Michigan.

Gerdel, R. W. and G. H. Strom. (1961). Scale Simulation of a Blowing Snow Environment. Proc. Inst. Environ. Sci., 53, 53-63.

Isyumov, N. (1971). An Approach to the Prediction of Snow Loads. Ph.D. Dissertation, University of Western Ontario, Ontario, Canada.
Iversen, J. D. (1979a). Drifting Snow Similitude. J. Hydraulics Division, Proceedings of the American Society of Civil Engineers, 105, HY6, 737-753.
Iversen, J. D. (1979b). Drifting Snow Similitude - Drift Deposit Rate Correlation. Fifth International Conference on Wind Engineering, Ft. Collins, Colorado, Proceedings, Paper VIII-6, 1.
Iversen, J. D. (1980). Drifting Snow Similitude - Transport Rate and Roughness Modeling. J. Glaciology, in press.
Kind, R. J. (1976). A Critical Examination of the Requirements for Model Simulation of Wind-Induced Erosion/Deposition Phenomena Such as Snow Drifting. Atmos. Environ., 10, 219-227.
Kind, R. J. and S. B. Murray. (1980). Saltation Flow Measurements Relating to Modeling of Snowdrifting, unpublished manuscript.
Kreutz, W. and W. Walter. (1956). Der Strömungsverlauf sowie die Erosionsvorgänge und Schneeablagerungen an künstlichen Windschirmen nach Untersuchungen un Windkanal. Berichte des Deutschen Wetterdienstes, 4, 24, 1-25.
Martinelli M. (1973). Snow Fence Experiments in Alpine Areas. J. Glaciology, 12, 65, 291-303.
Nϕkkentved, C. (1940). Drift Formation at Snow Fences. Stads-og Haveingenϕren, 31, 111-114.
Norem, H. (1975). Designing Highways Situated in Areas of Drifting Snow. Draft Translation 503, Cold Regions Research and Engineering Laboratory, Hanover, New Hampshire.
Odar, F. (1962). Scale Factors for Simulation of Drifting Snow. J. Engineering Mechanics Division, ASCE, 88, EM2, 1-16.
Odar, R. (1965). Simulation of Drifting Snow. Research Report 174, Cold Regions Research and Engineering Laboratory, Hanover, New Hampshire.
Ring, S. L., J. D. Iversen and J. B. Sinatra. (1979). Wind Tunnel Analysis of the Effects of Plantings at Highway Grade Separation Structures. Engineering Research Institute, Iowa State University, ISU-ERI-Ames 79221.
Sherwood, G. E. (1967). Preliminary scale model snowdrift studies using Borax in a wind duct. Technical Note N-682, Naval Civil Engineering Laboratory, Port Hueneme, California.
Strom, G. H., G. R. Kelly, E. L. Deitz and R. F. Weiss. (1962). Scale Model Studies on Snow Drifting. Research Report 73, U.S. Army Snow, Ice and Permafrost Research Establishment, Hanover, New Hampshire.
Tabler, R. D. and D. L. Veal. (1971). Effect of Snow Fence Height on Wind Speed. Bulletin of the International Association of Scientific Hydrology, 16, 49-56.
Tabler, R. F. (1973). New Snow Fence Design Controls Drifts, Improves Visibility, Reduces Road Ice. Proc. Annual Transp. Engr. Conf. 46, 16-27.
Tabler, R. D. (1974). New Engineering Criteria for Snow Fence Systems. Transp. Res. Record, 506, 65-78.
Tabler, R. D. (1977). Snow Control with Road Design and Snow Fences. Technical Institute on Snow Removal and Ice Control, University of Wisconsin, Madison.
Tabler, R. D. (1979). Geometry and Density of Drifts Formed by Snow Fences. Snow in Motion Symposium, Ft. Collins, Colorado.
Tabler, R. D. (1980a). Geometry and Density of Drifts Formed by Snow Fences. J. Glaciology, in press.
Tabler, R. D. (1980b). Self-similarity of wind profiles in blowing snow allows outdoor modeling. J. Glaciology, in press.
Tabler, R. D. and R. L. Jairell. (1980). Studying snowdrifting problems with small-scale models outdoors. Western Snow Conference, April 15-17, Laramie, Wyoming.
Theakston, F. A. (1970). Model Technique for Controlling Snow on Roads and Runways. Special Report 115, Cold Regions Research and Engineering Laboratory, Hanover, New Hampshire.